Thermal Shock Resistances of High Thermal Conductivity C/C-Composite as Plasma Facing Materials for Fusion Reactor Devices

著者	Sato S., Toida T., Teruyama K., Suzuki T.
journal or publication title	Science reports of the Research Institutes, Tohoku University. Ser. A, Physics, chemistry and metallurgy
volume	45
number	1
page range	99-104
year	1997-03-28
URL	http://hdl.handle.net/10097/28709

Sci. Rep. RITU A45 (1997) pp. 99-104
No. 1, March 1997

Thermal Shock Resistances of High Thermal Conductivity C/C−Composite as Plasma Facing Materials for Fusion Reactor Devices

S.Sato[a], T.Toida[b], K.Teruyama[c] and T.Suzuki[d]

[a] Faculty of Science and Engineering, Iwaki Meisei University, Iwaki,970, Japan and Training Center, The Japan Atomic Power Co., Tokai, Ibaraki,319−11, Japan

[b] Graduate School, Iwaki Meisei University, Iwaki, 970, Japan

[c] Hitachi Works, Hitachi Ltd., Hitachi, 317, Japan

[d] Hitachi Chemical Industries, Ltd., Sakuragawa, Hitachi, 316, Japan

(Received March 15, 1997)

The thermal shock resistances, mechanical and fracture mechanics properties of one directionally oriented carbon fiber reinforced carbon composite HUD−1S, which was recently developed as a plasma facing material for fusion reactor devices, are presented. These results are compared with the cases of a fine grain isotropic graphite PD−600S. HUD−1S has extremely high anisotropies, such as the thermal conductivity in the direction along the fiber orientation is extremely high in excess of the conductivity of copper or silver. But the conductivitics of normal directions are below a half of the case of graphite. The characteristic isotropies on the thermal shock resistances and fracture toughnesses of this composite are given quantitatively.

KEYWORDS : 1D C/C-composite, plasma facing material, anisotropy, thermal shock resistance, thermal shock fracture toughness.

1. Introduction

Graphite and carbon/carbon−composites have been used practically for the first wall materials for plasma confinement in fusion reactor devices, because of their excellent heat resistance and the thermal shock resistance properties. Recently to efficiently take off high heat generation in the first wall of a fusion reactor device, JT-60U,[1] a very high thermal conductivity uniaxial carbon fiber reinforced carbon composite HUD−1S (Hitachi Chemical Industries, Ltd.) has been developed in which the carbon fibers were oriented in one direction. This paper reports on experimental results of the anisotropies of the thermal shock resistances and the related mechanical and fracture mechanics properties of the HUD−1S for the purpose of evaluation of performance against thermal shock by the plasma disruptions. The obtained results are compared with the performance of a fine grain isotropic graphite PD−600S (Hitachi Chemical Industries, Ltd.) which is presently used as a part of plasma facing materials in the JT-60U.

2.Experimental Procedures

2.1 Experimental Materials

Table 1 shows the physical properties of the C/C−composite HUD−1S and graphite PD−600S. Photo 1 shows the directions A, B and C nominated to distinguish the characteristic anisotropy of the HUD−1S specimen and the surface structures in A-, B- and C-directions, respectively. HUD−1S is composed of two kinds of carbon fiber (a usual grade and a high elasticity grade). These fibers are arranged alternately in the condition of bundle. Since they differ the light reflection due to the kinds of fiber bundle, photographs of surfaces show stripe patterns changing tones of color at the interval of fiber bundle. The graphite PD−600S is an isotropic graphite made through isostatic molding. Anisotropies of HUD−1S are very large. The thermal conductivity of A-direction of HUD−1S is extremly high in excess of the conductivity of copper or silver. Besides, thermal conductivity in the hexagonal lattice plane of the graphite structure is said to be 2000 W/mK,[9] and is well over the value of 527 W/mK of A-direction of

Table 1 Physical properties of C/C HUD−1S and graphite PD−600S.

Material		HUD−1S (1−D)			PD−600S
		A (//)	B (⊥1)	C (⊥2)	
Density	[g/cm³]	1.85			1.80
Shore Hardness	[−]	33	34	33	60
Electrical Resistance	[μΩm]	2.5	25.8	43.6	12.0
Young's Modulus	[GPa]	300	5	4	12.0
Flexural Strength	[MPa]	372	12	8	53
Thermal Conductivity[1)]	[W/mk]	527	47	35	108
Thermal Expansion[2)]	[$\times 10^{-6}$/℃]	0	9.2	10.9	5.5

1) at 300 K, Laser flash method by Y.Gotoh(Hitachi Laboratory, Hitachi, Ltd.)

2) HUD−1S : R.T.~900℃, PD−600S : R.T.~700℃

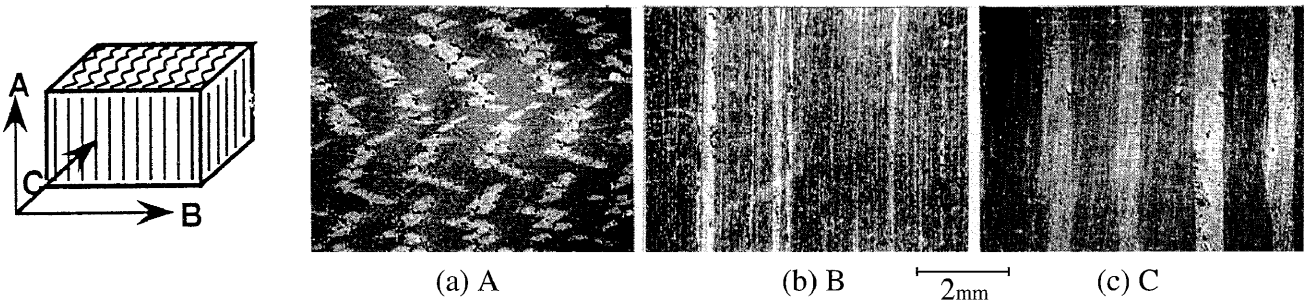

Photo 1 Surface structures in A-, B- and C-directions of HUD−1S (1−D C/C).

HUD−1S. The coefficient of thermal expansion of A-direction is zero at room temperature to 900℃. Young's modulus in A-direction is higher than the modulus of steel.

2.2 Experiments to determine the thermal shock resistance and the thermal shock fracture toughness.

Using disk specimens of radius R=10 mm, thickness h=2.0 mm, the thermal shock resistance, Δ, was determined by the measurement of the critical electric power W to cause thermal stress cracking at the periphery of disk by means of arc discharge heating of uniform heat flux at the central area of the heating radius ratio a/R=0.3. Using the same disk specimens machined previously having an edge slit of depth c=3.0 mm, the thermal shock fracture toughness, ∇, was also determined by the measurement of the critical electric power W to propagate the thermal stress cracking at the tip of the edge slit. The values of Δ and ∇ are determined by following equations, respectively.[(2),(3),(4),(5)]

$$\Delta = \sigma_t \lambda_t / E_{\alpha t} = S_1 \beta W / \pi h \,(a/R)^2 \qquad (1)$$

$$\nabla = K_{Ic} \lambda_t / E_{\alpha t} = F_1 \sqrt{\pi c}\, \beta W / \pi h \,(a/R)^2 \qquad (2)$$

where, σ_t is the tensile strength, λ_t is the thermal conductivity, E is Young's modulus, α_t is the coefficient of thermal expansion and K_{Ic} is the fracture toughness value of the mode I. S_1 is the maximum nondimensional thermal stress of circumferential direction at the periphery of the disk[(2),(3)] and is given by $S_1 = \sigma_{\theta max} / E_{\alpha t} Q$. Q is a function of temperature due to the electric heating for unit volume and is given by $Q = WR^2 / \lambda_t \pi a^2 h$. F_1 is the nondimensional stress intensity factor due to the thermal stress at the tip of the edge slit[(4),(5)] and is given by $F_1 = K_1 / \sqrt{\pi c}\, E_\alpha Q$, where K_I is the stress intensity factor at the tip of the edge slit. In this study, the edge slit was machined taking aim at the weakest direction of the anisotropy for the disk specimen of B- and C-directions. And β is a heating efficiency to be calibrated by the thermal shock testing apparatus. Characteristic values of S_1 and K_1 were originally obtained in the condition of homogeneious elastic bodies, but these values are assumed to be appicable to the anisotropic body in this study.

2.3 Experments of bending strength and fracture toughness

The bending strength, σ_b, was measured by the three points bending test for a beam of length l=60 mm, with a rectanglar cross section of width w =10 mm and height b =10 mm. The fracture toughness of the mode I, K_{Ic}, for the same beam with a central slit of depth c was also measured. They are expressed as follows;

$$\sigma_b = 3Ps/2wb^2 \qquad (3)$$

$$K_{IC} = f(\alpha)(Ps/wb^{3/2}) \qquad (4)$$

where P is the bending load, s is span length, f (α) is a function of α (= c /b).[6]

2.4 Young's modulus

Young's modulus E was determined by the measurement of ultrasonic pulse velocity for a rectangular rod specimen of a side length 10 mm and length l =150 mm for the direction A, and length l =60 mm for the B- and C-directions, using the following equation;

$$E = (\gamma/g)(l/t)^2 \qquad (5)$$

where γ is density, g is the accelaration of gravity and t is propagation time. Young's modulus at elevated temperatures was measured also by means of the ultrasonic method using intermediator rods of graphite for the rod specimen of A-direction inserted in a graphite tube to equalize the temperature up to 1000℃ in a tube type furnace.[7]

3. Expermental Results and Discussions

Table 2 shows the mean values of the experimental results of HUD−1S and PD−600S. Data are presented for thermal shock resistance, thermal shock fracture toughness, bending strength, fracture toughness, Young's modulus and equivalent crack size.

3.1 Thermal shock resistance and thermal shock fracture toughness

Figs.1 and 2 show electric powers in the thermal shock resistance test and the fracture toughness test for the three directions of the HUD−1S disk specimens, respectively. In these figures, open and solid circles show electric powers for non-fracture and fractured cases, respectively. The critical values of W were estimated from the middle points of the ranges of fractured and non-fracture points. The thermal shock resistance Δ and the fracture toughness ∇ calculated from the critical electric powers using the heating efficiency β =0.57〜0.67 were listed in Table 2. Photo 2(a),(b) and (c) show typical fracture appearances in the thermal shock resistance test of HUD−1S. The characteristic differences between B- and C-directions are not found. Photo 3(a) and (b) show typical cracking paths from the outer peripheries of the disk specimens. Photo 4(a),(b) and (c) show typical fracture appearances in the thermal shock fracture toughness tests of A-,B- and C-direction of HUD−1S. Photo 5(a) and (b) show cracking from the tip of edge slit of the disk specimen

Table 2 Mean values of the experimental results of HUD−1S and PD−600S

Material	HUD−1S (1−D)			PD−600S
	A (//)	B (⊥1)	C (⊥2)	
Thermal shock resistance Δ (W/mm)	8.6	52.1	77.2	37.0
Thermal shock fracture toughness ∇ (W/mm$^{1/2}$)	46.8	164	174	35.3
Bending strength σ_b (MPa)	111	8.4	7.7	71
Mode I fracture toughness K_{IC} (MPam$^{1/2}$)	9.69	0.42	0.38	1.01
Young's modulus E (GPa)	297	4.5	3.6	10.1
Equivarent crack length (mm) $C_{e1}=\pi^{-1}(\nabla/\Delta)^2$	9.43	3.13	1.62	0.29
Equivarent crack length (mm) $C_{e2}=\pi^{-1}(K_{Ic}/\sigma_b)$	5.45	1.77	1.74	0.14

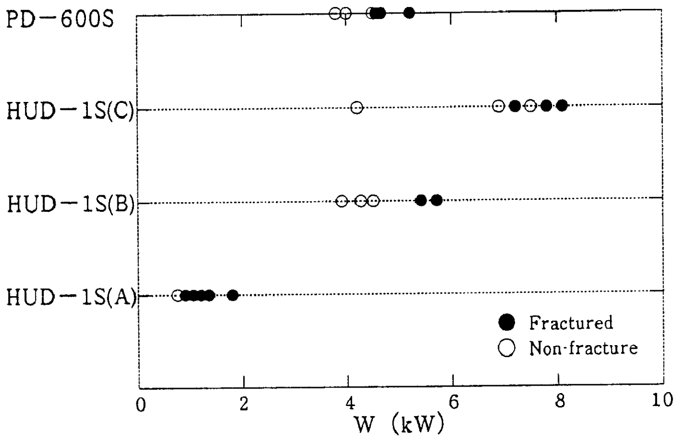

Fig.1 Electric powers in the Thermal shock resistance tests of HUD−1S and PD−600S

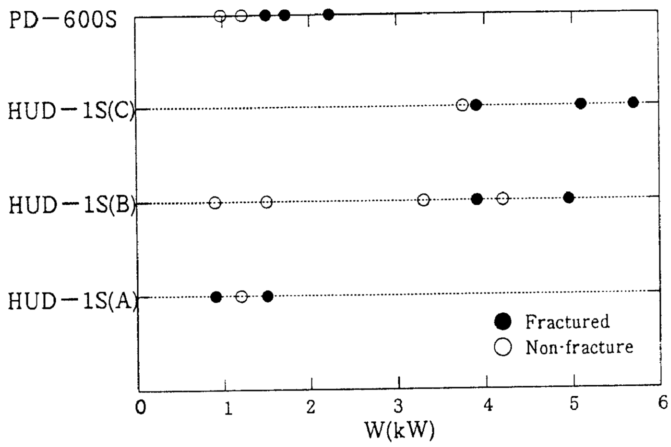

Fig.2 Electric powers in the Thermal shock fracture toughness tests of HUD−1S and PD−600S

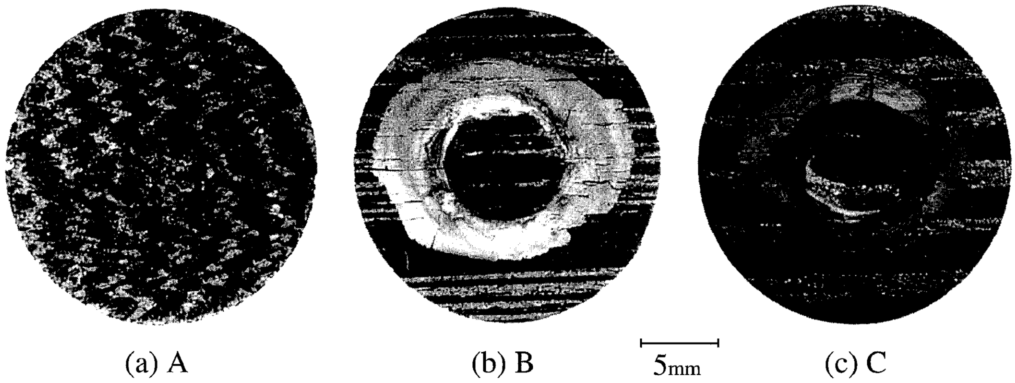

Photo 2 Typical fractures in the thermal shock resistance test of HUD−1S.

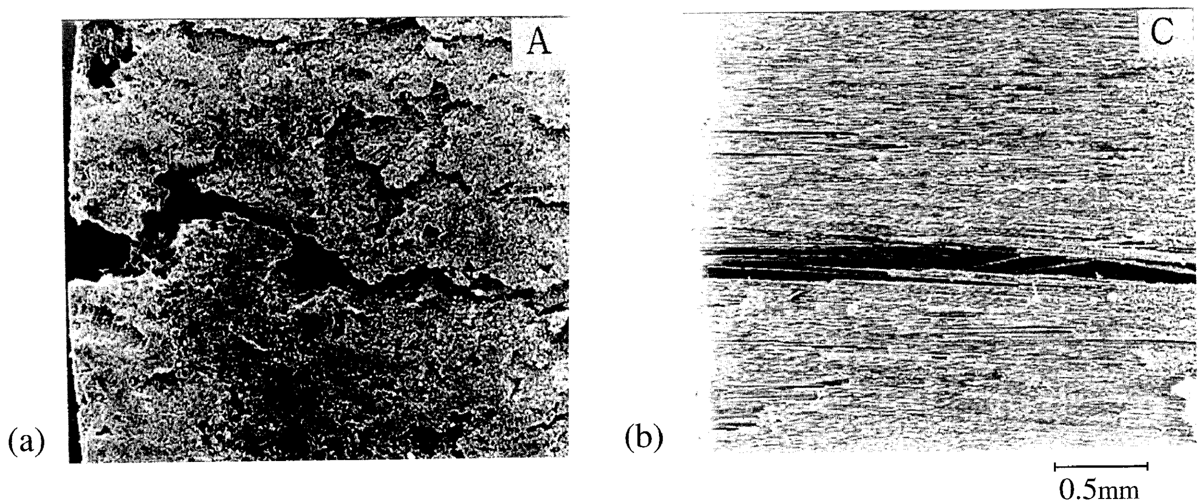

Photo 3 Typical crack propagation from the periphery of disk specimen in the thermal shock resistance test of HUD−1S.

A- and B-direction, respectively.

The values of ⊿ and ∇ of A-direction of HUD−1S along the fiber orientation are very small, reflecting the small thermal conductivity in the radial direction of the disk specimen corresponding to the B- and C-directions. On the other hand, the values ⊿ and ∇ for B- and C-direction of HUD−1S show the weakest ones in the high anisotropy of the disk specimens. But the values of B- and C-direction of HUD−1S are comparatively large, since the thermal conductivites are high for favorable direction of the fiber arrangements.

3.2 Bending strength and fracture toughness

The bending strength and fracture toughness for A-direction of HUD−1S are relatively large, since the fiber orientation as along the longitudinal axis of the

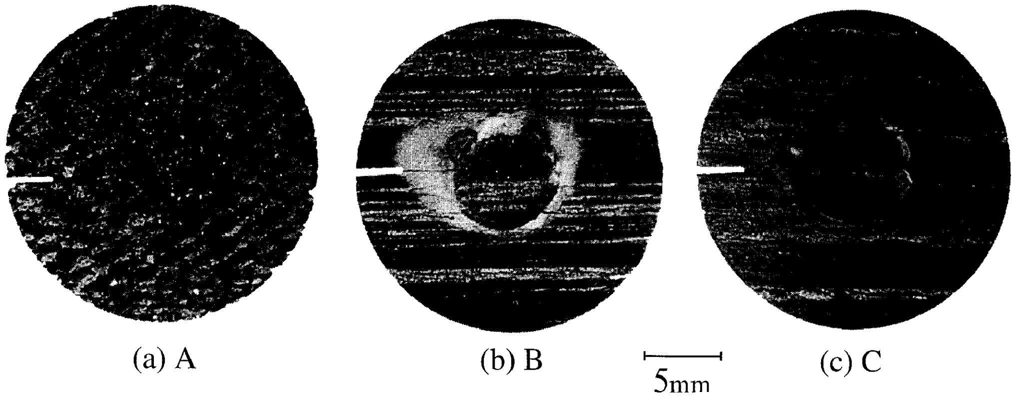

Photo 4　Typical fractures in the thermal shock fracture toughness test of HUD－1S.

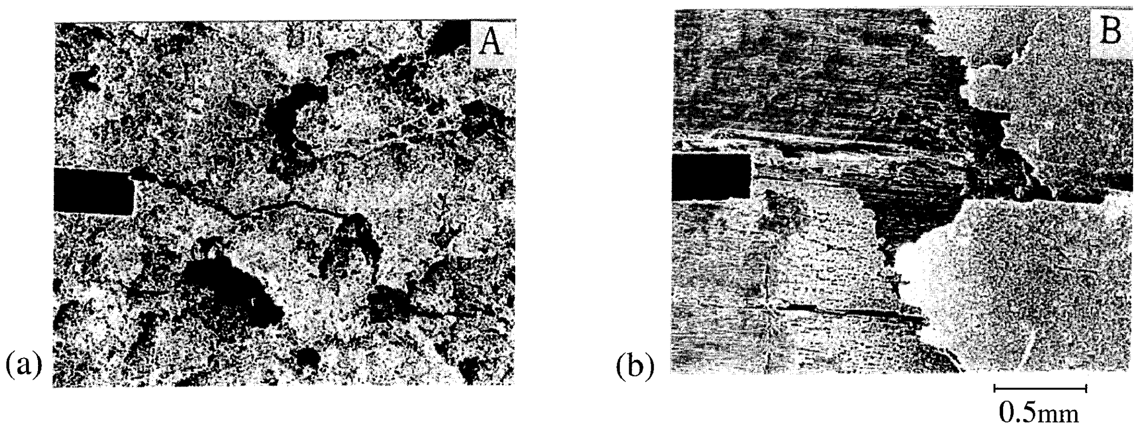

Photo 5　Typical crack propagation from the tip of edge slit in the thermal shock fracture toughness test of HUD－1S.

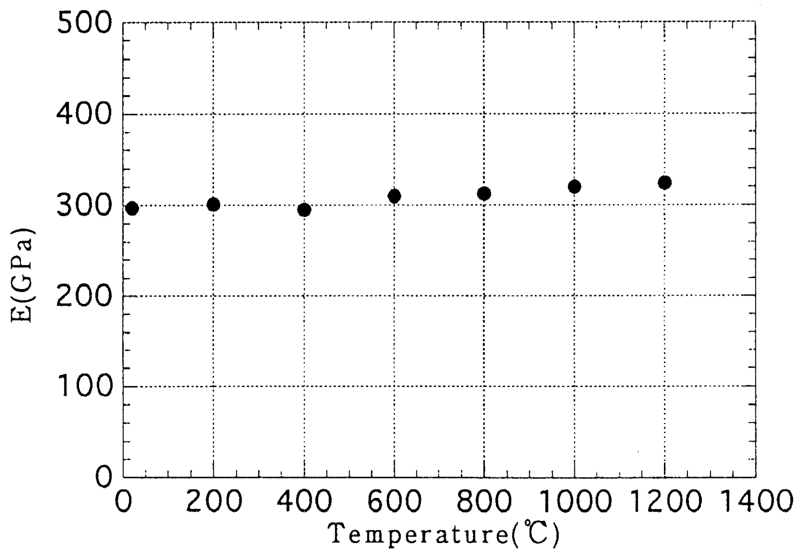

Fig.3　Young's modulus of the C/C-composite HUD－1S, A(//) at elevated temperature

rod specimens. By comparison, the values for B- and C-direction of HUD－1S (C) are found to be very weak, extraordinarily less than one order of the magnitude in A-direction.

3.3 Young's modulus

Fig.3 shows the Young's modulus of A-direction of HUD－1S as a function of temperature up to 1000℃. The modulus is found to increase slightly with increase in temperature. This value is about 30 times of the case of graphite PD－600S. By comparison, the values of B- and C-direction of HUD－1S are very much smaller, less than two orders than in the A-direction, since the ultrasonic pulses pass transversely in the fiber boundaries and the propagation speeds are slow compared with the A-direction. The Young's modulus of PD−600S is about twice of B- and C-direction of HUD−1S.

3.4 Equivalent crack size

This value corresponds to a half size of a small penetrated crack in an infinitely wide plate of the fracture toughness K_{IC}, subjected to normal intensity of the tensile strength σ_t, namely

$$C_{e1} = \pi^{-1}(K_{IC}/\sigma_t)^2 \qquad (6)$$

Tensile strength σ_t in equation (6) was approximately estimated from the bending strength σ_b as $\sigma_t \fallingdotseq \sigma_b/1.5$ using the statistical approach based on Weibull's theory.[8]

The equivalent crack size is also expressed similarly for the thermal stress fracture as

$$C_{e2} = \pi^{-1}(\nabla/\Delta)^2 \qquad (7)$$

The values of C_{e1} and C_{e2} of A-direction of HUD−1S are fairly large, to allow the defect in the material to be visible to inspection. On the other hand, the Ce's for PD−600S are very small, showing high crack sensitivity.

4.Conclusions

For effective heat absorption of plasma-facing wall in fusion reactor devices, development of high thermal conductivity materials has been emphatically demanded. In this study on a uniaxially oriented carbon fiber carbon composite HUD−1S, we have evaluated experimentally the thermal shock resistances against plasma disruptions including the mechanical and fracture mechanics properties. HUD−1S showed extremly high anisotropies as is easily presumed from the manufacturing process of fiber arrangement. Thermal conductivities of HUD−1S in A-direction along the fiber was a very high as surpassing conductivities of silver and copper, but the nomal B- and C-directions were no more than a half of graphite PD−600S.

As plasma-facing materials, the surface of A-direction is properly subjected severe thermal shocks due to plasma disruptions. The thermal shock resistance and the thermal shock fracture toughness in A-direction were found to be considerably small on account of very low thermal conductivities, mechanical strengths and fracture toughnesses, and large Young's moduli and coefficients of thermal expansion in B- and C-directions normal to the surface.

This uniaxtally oriented high thermal conductivity carbon fiber composite; HUD−1S is considered concludingly to come into serious question in concerned cases with multi-axial properties such as thermal shock due to plasma disruption on the surface, because of the excessive anisotropy in use practically as plasma-facing wall materials for fusion reactor devices.

References

1) H.Ikegami, et al.,Ed: Fusion Reactor Engineering, Nagoya University Press. Part 2 (1995), p.413〜634.
2) S.Sato, et al., : Carbon. 13 (1975) p.309〜316.
3) S.Sato, et al., : Research Bull, Collge of Sci. and Eng., Iwaki Meisei Univ., No.8(1995) p.60〜69.
4) S.Sato, et al., : Carbon. 16 (1978) p.103〜109.
5) S.Sato, et al., : Research Bull, Collge of Sci. and Eng., Iwaki Meisei Univ., No.8(1995) p.70〜81.
6) JSME S 001 (1981) p.19.
7) S.Sato, et al., : Carbon. 2 (1964) p.309〜316.
8) S.Sato: Symposium on Carbon. Tokyo V-5 (1964).
9) S.Tanuma, et al., : Modern Knowledge of Elements, Tokyo Shoseki Co. (1975) p.20.